Session I - 1.4

FILAMENT ENVIRONMENT

https://doi.org/10.1017/S1743921313010855 Published online by Cambridge University Press

Nature of Prominences and their role in Space Weather
Proceedings IAU Symposium No. 300, 2013
B. Schmieder, J.-M. Malherbe & S. T. Wu, eds.

doi:10.1017/S1743921313010855

Structure and Topology of Magnetic Fields in Solar Prominences

Adriaan A. van Ballegooijen[1] and Yingna Su[1]

[1]Harvard-Smithsonian Center for Astrophysics,
60 Garden Street MS-15, Cambridge, MA 02138, USA
email: vanballe@cfa.harvard.edu

Abstract. Recent observations and models of solar prominences are reviewed. The observations suggest that prominences are located in or below magnetic flux ropes that lie horizontally above the PIL. However, the details of the magnetic structure are not yet fully understood. Gravity likely plays an important role in shaping the vertical structures observed in quiescent prominences. Preliminary results from a time-dependent model describing the interaction of a magnetic flux rope with photospheric magnetic elements are presented.

Keywords. Sun: prominences, Sun: filaments, Sun: magnetic fields

1. Observations

In this section we present an overview of various observations relevant to the magnetic structure of solar prominences. For more detailed reviews, see Tandberg-Hanssen (1995), Labrosse *et al.* (2010) and Mackay *et al.* (2010).

Filament channels: It is well known that filaments are located above polarity inversion lines (PIL) in the photospheric magnetic field (e.g., Babcock & Babcock 1955; Howard 1959). Most filaments are located within channels, traditionally defined as corridors surrounding PILs where the chromospheric Hα fibrils are aligned with the PIL (e.g., Martres *et al.* 1966; Foukal 1971; Gaizauskas *et al.* 1997; Gaizauskas *et al.* 1998; Martin 1998). This fibril alignment implies that at chromospheric heights the magnetic field is dominated by its component along the PIL, and suggests the presence of a horizontal magnetic flux bundle in the low corona above the channel. The magnetic field in this flux bundle is highly sheared in the direction along the PIL, but may have some twist consistent with the direction of the overlying arcade field. The base of the (weakly twisted) flux bundle lies on the chromosphere, so the direction of its magnetic field is imprinted on the chromospheric fibrils. Filament channels can be classified as either *dextral* or *sinistral* depending on the direction of the magnetic field along the PIL as seen by an observer standing on the positive-polarity side of the channel (Martin *et al.* 1992). The chirality of filament channels can also be inferred from the plume-like tails of coronal emission cells observed with instruments on the Solar Dynamics Observatory (SDO) and the Solar Terrestrial Relations Observatory (STEREO) spacecraft (Sheeley *et al.* 2013). Filament channels exhibit a strong hemispheric pattern: those in the north are dominantly dextral, and those in the south are dominantly sinistral (Martin *et al.* 1994; Zirker *et al.* 1997).

The above view of a filament channel as a weakly twisted flux bundle lying on the chromosphere may apply to most low- and mid-latitude filaments, but may not be correct for polar crown prominences. At the polar crown PILs the chromospheric fibrils are nearly randomly oriented, even when prominences are present at larger heights. Therefore, the alignment of chromospheric fibrils is apparently not a necessary requirement for prominence formation. We suggest that the flux bundles supporting polar crown prominences may be somewhat elevated above the chromosphere, so that they have little effect on the

chromospheric fibrils. Therefore, we will use the term "filament channel" also for polar crown prominences, even though alignments of chromospheric fibril along the PIL are not observed in this case.

Filament environment: In disk observations the filament channels appear as voids in coronal soft X-ray emission (e.g., Engvold 1989). EUV channels are darker than their surroundings, which may be due to a combination of lower emission in the channel and absorption of EUV line radiation in the H I Lyman continuum (Heinzel *et al.* 2001; Schmieder *et al.* 2003). In off-limb observations the channels appear as relatively dark coronal cavities surrounding the prominence. These cavities can be seen in white light coronagraph observations (Gibson *et al.* 2006), and also in the EUV and soft X-rays (e.g., Hudson *et al.* 1999). The cavity is located in the lower part of a helmet streamer that extends far from the Sun. Régnier *et al.* (2011) observed coronal plasma on U-shaped magnetic field lines sitting at the bottom of a cavity located above the polar crown. This U-shape of the field lines is consistent with the presence of a large flux rope supporting the prominence. Coronal cavities can support complex internal flows (Schmit *et al.* 2009; Wang & Stenborg 2010), indicating that the flux rope is not in a steady state. Rotational motions are also observed during eruptions (e.g., Panasenco *et al.* 2012). Immediately outside the cavity is an arcade of coronal loops that prevent the filament flux rope from expanding into the heliosphere, hence these loops play an important role in the overall force balance of the flux rope.

Su *et al.* (2010) presented observations of filament channels on the quiet Sun, and found a distinct asymmetry in the morphology of the bright structures on the two sides of the channel (also see Sheeley *et al.* 2013). As shown in Figure 1, one side of the channel has curved features, while the other side has straight features. This asymmetry is thought to be due to a variation in axial flux along the channel, which causes the field lines from one polarity to turn into the flux rope (curved features) while the field lines from the other polarity are connected to distant sources (straight features).

Spectro-polarimetry: The most direct way of studying the prominence magnetic fields is by inverting spectro-polarimetric data from Zeeman-sensitive spectral lines (e.g., Paletou & Aulanier 2003; López Ariste & Aulanier 2007). For example, the He I 1083.0 nm triplet is sensitive to the joint action of atomic level polarization (generated by anisotropic radiation pumping), the Hanle effect (modification of atomic level polarization due to a magnetic field) and the Zeeman effect (Lin *et al.* 1998; Trujillo Bueno *et al.* 2002; Orozco Suárez *et al.* 2013). Measurements using the He I 587.6 nm (D3) line above the solar limb have shown that the magnetic field strengths in quiescent prominences are in the range 3 - 15 G (Leroy 1989). The field is mostly horizontal and makes an angle of about 40° with respect to the long axis of the prominence (Bommier & Leroy 1998). The field strength increases slightly with height, indicating the presence of dips in the field lines. Most prominences have inverse polarity, i.e., the component of magnetic field perpendicular to the prominence long axis has a direction opposite to that of the potential field. The component along the prominence axis exhibits the hemispheric pattern discussed above (Leroy *et al.* 1983). Using full-Stokes polarimetry, Casini *et al.* (2003) were the first to make a map of the vector field in a prominence. Their results are consistent with the earlier measurements by Leroy and collaborators, but they also found localized regions with strong magnetic field (up to 80 G) within the prominence. Merenda *et al.* (2006) observed a polar crown prominence above the limb and found evidence for a magnetic field oriented only 25° from the vertical.

Spectro-polarimetry can also be applied on the solar disk. For example, Kuckein *et al.* (2012) observed an active region filament simultaneously in the photosphere and chromosphere. They found that the inferred vector fields are consistent with the presence

https://doi.org/10.1017/S1743921313010855 Published online by Cambridge University Press

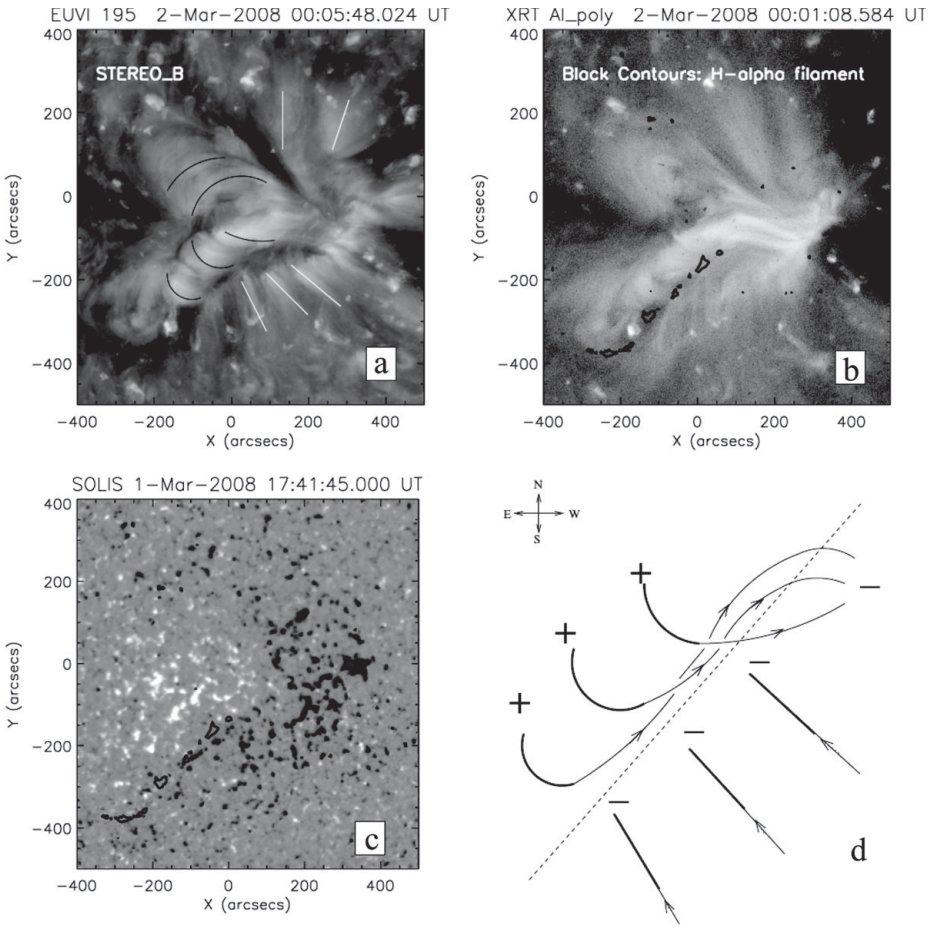

Figure 1. Asymmetry of coronal structures near filament channels. (a) STEREO/EUVI image of a channel observed on 2008 March 2 in the 195 Å passband. The bright features on the east side (black) are curved into the channel, while those on the west side (white) are more straight and point away from the channel. (b) Hinode/XRT image shows sheared loops overlying the channel; black contours indicate location of Hα filament. (c) Photospheric magnetogram taken by NSO/SOLIS on previous day. (d) Interpretation of curved structures in terms a model in which the axial magnetic flux increases in NW direction along the PIL (dotted line). Adapted from Su *et al.* (2010).

of a magnetic flux rope that lies at low heights in the solar atmosphere. Yelles Chaouche *et al.* (2012) used these observations to construct a non-linear force-free field (NLFFF) model for the filament.

Filament fine structures: When observed on the solar disk with high spatial resolution, filaments show thin thread-like structures that continually evolve (Lin *et al.* 2008). A typical solar filament is composed of a spine, barbs, and two extreme ends. The spine defines the upper horizontal part of a filament, and the barbs are lateral extensions that extend from the spine to the chromosphere below (e.g., Martin 1998; Lin 2011). Active region filaments consist of narrow spines without barbs, intermediate filaments have a combination of both a spine and barbs, and quiescent filaments are dominated by barbs and vertical threads. When viewed from above, the barbs are either right-bearing or

https://doi.org/10.1017/S1743921313010855 Published online by Cambridge University Press

left-bearing, like ramps off a highway (Martin *et al.* 1992). There is a strong correlation between the orientation of the barbs and the chirality of the filament channel: filaments in dextral channels usually have right-bearing barbs, and those in sinistral channels usually have left-bearing barbs. At present the cause of this relationship is not well understood. Recently, Liu *et al.* (2010) found some cases where the barbs change their orientation within a period of a few hours, indicating there are exceptions to the above rule. Martin & Echols (1994) proposed that the barbs are rooted in parasitic polarity elements in the photosphere, and Aulanier *et al.* (1998) showed that the barbs move in accordance with the changes in the parasitic polarities. Others have argued that the ends of the barbs are located near small-scale PILs between majority and minority polarities (Wang 1999; Chae *et al.* 2005; Lin *et al.* 2005). Flux cancellation between parasitic polarities and the neighboring dominant polarity is believed to play an important role in the formation of the barbs (Wang 2001; Wang & Muglach 2007).

Recent observations with the Solar Optical Telescope on the Hinode satellite have revolutionized our understanding of quiescent and intermediate prominences. When observed above the solar limb, such prominences always show many thin thread-like structures. In some cases the threads are mainly horizontal (e.g., Okamoto *et al.* 2007), in other cases they are mainly vertical (e.g., Berger *et al.* 2008; Berger *et al.* 2010; Chae *et al.* 2008; Chae 2010). The horizontal threads may be understood as plasma being supported at the dips of weakly twisted, nearly horizontal field lines, but the structure of the vertical threads is not yet fully understood. The vertical threads are often not clearly visible (or not recognized) in on-disk Hα observations; to see them on the disk requires high-resolution observations in other passbands, such as SDO/AIA 171 Å. Hedgerow prominences consist of many thin vertical threads organized in a vertical sheet or curtain. Upward-moving plumes and bubbles have been observed in between the denser, downflowing threads (e.g., Berger *et al.* 2008). Other prominences consist of isolated dark columns standing vertically above the PIL, and such prominences often exhibit rotational motions reminicent of "tornados" in the Earth's atmosphere (e.g., Su *et al.* 2012; Li *et al.* 2012; Panesar *et al.* 2013). The rotational motions have been confirmed using Doppler shift measurements (e.g., Liggett & Zirin 1984; Orozco Suárez *et al.* 2012). Some quiescent prominences have horn-like extensions that protrude from the top of the spine into the cavity above (e.g., Berger 2012; Schmit & Gibson 2013). These horns may outline a flux rope located above the prominence (Berger 2012).

2. Prominence Models

The cool prominence plasma must somehow be supported against gravity because without such support the plasma would fall to the chromosphere on a time scale of about 10 minutes. It has long been assumed that prominences are threaded by horizontal magnetic fields and electric currents, which provide the upward Lorentz force needed to counter gravity (e.g., Kippenhahn & Schlüter 1957; Kuperus & Raadu 1974; Pneuman 1983). However, the global topology of the magnetic field threading the prominence is not yet understood. For example, for tornado-like prominences it is unclear how horizontal fields can survive in the presence of rotational motions of the vertical structures (Liggett & Zirin 1984).

To understand the global structure of the filament magnetic field, Martin & Echols (1994) and Lin *et al.* (2008) proposed a conceptual model in which the filament plasma is located on arched field lines that extend along the length of the filament. The longest field lines represent the spine, and shorter ones splay sideways on both sides of the filament to form the barbs. In this model the barbs are located on inclined field lines,

https://doi.org/10.1017/S1743921313010855 Published online by Cambridge University Press

so this model does not explain how the plasma is supported against gravity. Aulanier *et al.* (1998) argued that filaments are located in weakly twisted flux ropes overlying the PIL. The filament plasma is located at dips in the field lines, and the barbs represent local distortions of the flux rope, causing the dips to be displaced from the main filament path. These distortions are due to parasitic polarities or bipoles in the photosphere below the filament channel (also see Dudik *et al.* 2012). Lionello *et al.* (2002) presented a data-driven MHD model describing the formation of an observed active region filament. They showed that the magnetic flux changes in the photosphere can produce a flux rope at the appropriate location, and that plasma condensations can form at the dips of the field lines. Su & van Ballegooijen (2012) developed a NLFFF model of a quiescent prominence observed with SDO and STEREO, and found that the flux rope has magnetic connections with the surrounding quiet Sun. Other variants of the flux rope model are the quadrupolar model (Magara *et al.* 2011) and the double-decker filament model (Liu *et al.* 2012).

It seems likely that gravity plays an important role in shaping the observed vertical structures. Berger *et al.* (2008) and Hillier *et al.* (2012) argued that the observed structures must be the result of a Rayleigh-Taylor (RT) instability. Van Ballegooijen & Cranmer (2010) proposed that hedgerow prominences are located in vertical current sheets, and that the plasma is supported by small-scale "tangled" magnetic fields within the sheet. Berger (2012) proposed the current sheet is located below an elevated flux rope (also see Fan 2012). One problem with these ideas is that small-scale tangled fields are not consistent with the apparent smoothness of the magnetic fields derived from Hanle measurements (e.g., Orozco Suárez *et al.* 2013). Haerendel & Berger (2011) suggested that the observed downflows may consist of plasma packets that squeeze themselves through the dominantly horizontal field under the action of gravity (also see Low *et al.* 2012b). Low *et al.* (2012a) investigated the coupling between the force balance and energy transport in quiescent prominences, and they suggest that the vertical threads may be falling across magnetic fields, with optically thick cores much denser and less ionized than conventionally assumed. Hillier & van Ballegooijen (2013) developed a 2.5D model for the support of prominence material by the dips of a coronal flux rope, and found that the magnetic field is significantly distorted by the weight of the prominence plasma. For some magnetic configurations force balance may not be possible unless the ratio of gas- and magnetic pressures is quite small, $\beta < 0.1$. This is opposite to Hillier *et al.* (2012), who need $\beta > 0.1$ to obtain RT instability.

Luna *et al.* (2012) simulated the formation and evolution of a multi-threaded solar prominence inside a flux rope. The process is governed by thermal nonequilibrium of the coronal plasma. They find that the condensations in the corona can be divided into two groups: threads and blobs. Threads are massive condensations that linger in the dips of the field lines, while blobs are small condensations that rapidly fall to the chromosphere. This model holds great promise for understanding how mass is supplied to the prominence. Models for the radiation emitted by prominence plasmas supported in magnetic dips have been developed by many authors (see Berlicki *et al.* 2011, Gunár *et al.* 2013, and references therein).

The observed hemispheric pattern of chirality (Zirker *et al.* 1997) has been investigated using models for the coupled evolution of the photospheric and coronal magnetic fields (see Mackay *et al.* 2010, and references therein). Recently, Yeates & Mackay (2012) simulated the evolution of the magnetic field over a full solar cycle. This model includes the effects of solar differential rotation, meridional flows and supergranular diffusion on the surface magnetic field, and new active regions are injected into the model in accordance with observed magnetograms (synoptic maps from NSO Kitt Peak). The modeled corona evolves through a series of nearly force-free equilibrium states, and coronal flux

https://doi.org/10.1017/S1743921313010855 Published online by Cambridge University Press

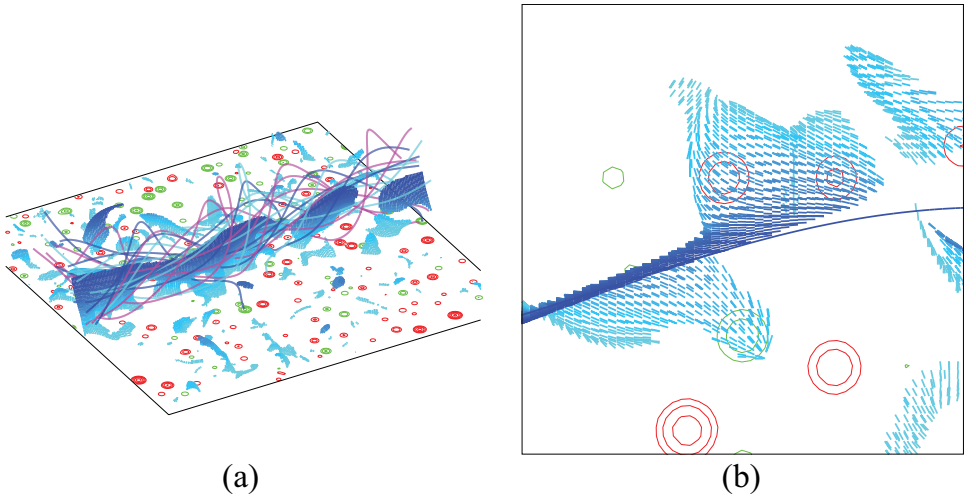

Figure 2. Model for the interaction of magnetic elements with a twisted flux rope. (a) Magnetic field at time $t = 200$ hrs. The red (green) features are positive (negative) magnetic flux elements on the photosphere. The colored curves are selected field lines within the flux rope (overlying field not shown). The blue feature are dips in the field lines (darkness increases with height). The front side is dominantly positive polarity (red) but has many parasitic (green) elemnts. (b) Close-up of several right-bearing "barbs" that formed when magnetic elements crossed the PIL.

ropes develop over the PILs. The predicted chirality of these flux ropes is compared with the observed hemispheric pattern. The authors find that differential rotation can lead to opposite chirality at high latitudes, but only for about 5 years of the solar cycle following the polar field reversal. At other times the transport of magnetic helicity from lower latitudes overcomes the effect of *in situ* differential rotation, producing the majority chirality even on the polar crowns (Yeates & Mackay 2012). These results indicate that helicity transport from lower latitudes is important for understanding the hemispheric pattern of filament chirality, and that the corona has long-term memory of its helicity.

Recently, we developed a model describing the interaction of a coronal flux rope with magnetic elements in the photosphere. The evolution of the coronal magnetic field is simulated using the magneto-frictional method (e.g., van Ballegooijen *et al.* 2000). The time-dependent boundary conditions include the effects of emerging bipoles, as well as random motion, splitting, merging and cancellation of magnetic flux elements. The initial field contains a dextral flux rope with left-helical twist. Figure 2a shows a perspective view of the flux rope after 200 hours solar time. The blue features are the field-line dips in the lower half of the twisted flux rope. The curtain of dips is highly distorted by parasitic polarities below the flux rope, resulting in barb-like extensions. A close-up view from above (Figure 2b) shows that the barbs are right-bearing for this dextral channel. Therefore, the model reproduces the observed relationship between dextral (sinistral) channels and right (left) bearing barbs (Martin *et al.* 1992), consistent with earlier results from LFFF models (Aulanier *et al.* 1998).

In summary, various observations suggest that solar prominences are located in magnetic flux ropes that lie horizontally above the PIL. For active region filaments these flux ropes are thin and almost untwisted; for intermediate and quiescent filaments some twist seems to be required by the spectro-polarimetric measurements. The plasma may be supported by dips in the field lines. Models for the 3D magnetic fields in and around

https://doi.org/10.1017/S1743921313010855 Published online by Cambridge University Press

prominences have been developed using various techniques (e.g., NLFFF and MHD models). Including the weight of the prominence plasma into such models is difficult because the pressure scale height of the prominence plasma ($H_p \approx 300$ km) is much smaller than the typical size of the flux rope. Therefore, modeling quiescent prominences represent a challenging computational problem.

Acknowledgements: This project is supported by NASA grant NNX12AI30G as well as NASA contract SP02H1701R from LMSAL to SAO.

References

Aulanier, G., Démoulin, P., van Driel-Gesztelyi, L., Mein, P., & Deforest, C. 1998, *A&A*, 335, 309

Babcock, H. W. & Babcock, H. D. 1955, *ApJ*, 121, 349

Berger, T. E. 2012, in Second ATST-EAST Meeting: Magnetic Fields from the Photosphere to the Corona, eds. T. R. Rimmele, M. Collados, *et al.*, ASP Conf. Series, Vol. 463 (Astron. Soc. of the Pacific, San Francisco), p.147

Berger, T. E., Shine, R. A., Slater, G. L., *et al.* 2008, *ApJ*, 676, L89

Berger, T. E., Slater, G., Hurlburt, N., *et al.* 2010, *ApJ*, 716, 1288

Berlicki, A., Gunár, S., Heinzel, P., Schmieder, B., & Schwartz, P. 2011, *A&A*, 530, A143

Bommier, V. & Leroy, J.-L. 1998, in New Perspectives on Solar Prominences, IAU Colloq. 167, eds. D. Webb, D. Rust, B. Schmieder, ASP Conf. Series, Vol. 150 (Astron. Soc.of the Pacific, San Francisco), p. 434

Casini, R., Löpez Ariste, A., Tomczyk, S., & Lites, B. W. 2003, *ApJ*, 598, 67

Chae, J., Moon, Y.-J., & Park, Y.-D. 2005, *ApJ*, 626, 574

Chae, J., Ahn, K., Lim, E.-K., Choe, G. S., & Sakurai, T. 2008, *ApJ*, 689, L73

Chae, J. 2010, *ApJ*, 714, 618

Engvold, O. 1989, in Dynamics and Structure of Quiescent Solar Prominences, ed. E. R. Priest (Kluwer, Dordrecht), p.47

Fan, Y. 2012, *ApJ*, 758, 60

Foukal, P. 1971, *Sol. Phys.*, 19, 59

Gunar, S., Mackay, D. H., Anzer, U., & Heinzel, P. 2013, *A&A*, 551, id.A3

Gaizauskas, V., Zirker, J. B., Sweetland, C., & Kovacs, A. 1997, *ApJ*, 479, 448

Gaizauskas, V. 1998, in New Perspectives on Solar Prominences (ASP Conference Series, Vol. 150, IAU Colloquium 167), eds. D. Webb, D. M. Rust, & B. Schmieder, p.257

Gibson, S. E., Foster, D., Burkepile, J., de Toma, G., & Stanger, A. 2006, *ApJ*, 641, 590

Haerendel, G. & Berger, T. 2011, *ApJ*, 731, 82

Heinzel, P., Schmieder, B., & Tziotziou, K. 2001, *ApJ*, 561, L223

Hillier, A., Berger, T., Isobe, H., & Shibata, K. 2012, *ApJ*, 746, 120

Hillier, A. & van Ballegooijen, A. A. 2013, *ApJ*, 766, 126

Howard, R. 1959, *ApJ*, 130, 193

Hudson, H. S., Acton, L. W., Harvey, K. L., & McKenzie, D. E. 1999, *ApJ*, 513, L83

Kippenhahn, R. & Schlüter, A. 1957, *Z. Astrophys.*, 43, 36

Kuckein, C., Martinez Pillet, V., & Centeno, R. 2012, *A&A*, 539, A131

Kuperus, M. & Raadu, M. A. 1974, *A&A*, 31, 189

Labrosse, N., Heinzel, P., Vial, J.-C., Kucera, T., Parenti, S., Gunár, S., Schmieder, B., & Kilper, G. 2010, *Space Sci Rev*, 151, 243

Leroy, J.-L. 1989, in Dynamics and Structure of Quiescent Solar Prominences, ed. E. R. Priest (Kluwer, Dordrecht), p.77

Leroy, J.-L., Bommier, V., & Sahal-Brechot, S. 1983, *Sol. Phys.*, 83, 135

Li, X., Morgan, H., Leonard, D., & Jeska, L. 2012, *ApJ*, 752, L22

Liggett, M. & Zirin, H. 1984, *Sol. Phys.*, 91, 259

Lionello, R., Mikić, Z., Linker, J. A., & Amari, T. 2002, *ApJ*, 581, 718

Lin, H., Penn, M. J., & Kuhn, J. R. 1998, *ApJ*, 493, 978

Lin, Y., Engvold, O., Rouppe van der Voort, L., Wiik, J. E., & Berger, T. E. 2005, *Sol. Phys.*, 226, 239

Lin, Y., Martin, S. F., & Engvold, O. 2008, in Subsurface and Atmospheric Influences of Solar Activity, ed. R. Howe, R. W. Komm, K. S. Balasubramaniam, & G. J. D. Petrie, ASP Conf. Series, Vol. 333 (Astron. Soc. of the Pacific), p. 235

Lin, Y. 2011, *Space Sci. Rev.*, 158, 237

Liu, R., Xu, Y., & Wang, H. 2010, *Mem. S. A. It.*, Vol. 81, 796

López Ariste, A. & Aulanier, G. 2007, in The Physics of the Chromospheric Plasmas, ed. P. Heinzel, I. Dorotovic, R. J. Rutten, ASP Conf. Series, Vol. 368 (Astron. Soc. of the Pacific, San Francisco), p. 291

Low, B. C., Berger, T., Casini, R., & Liu, W. 2012a, *ApJ*, 755, 34

Low, B. C., Liu, W., Berger, T., & Casini, R. 2012b, *ApJ*, 757, 21

Luna, M., Karpen, J. T., & DeVore, C. R. 2012, *ApJ*, 746, 30

Magara, T., An, J.-M. Lee, H., & Kang, J. 2011, *J. Korean Astron. Soc.*, 44, 143

Mackay, D. H., Karpen, J. T., Ballester, J. L., Schmieder, B., & Aulanier, G. 2010, *Space Sci Rev*, 151, 333

Martin, S. F. 1998, *Sol. Phys.*, 182, 107

Martin, S. F., Billamoria, R., & Tracadas, P. W. 1994, in Solar Surface Magnetism, eds. R. J. Rutten, & C. J. Schrijver, Kluwer Academic Pubishers, Dordrecht, Holland, 303

Martin, S. F. & Echols, Ch.R. 1994, in Solar Surface Magnetism, eds. R. J. Rutten & C. J. Schrijver, Kluwer Academic Pubishers, Dordrecht, Holland, 339

Martin, S. F., Marquette, W., & Billamoria, R. 1992, in The Solar Cycle, ed. K. Harvey, Proceedings of the 12th Summer Workshop, National Solar Observatory, 53

Martres, M.-J., Michard, R., & Soru-Iscovici, I. 1966, *A&A*, 29, 249

Merenda, L., Trujillo Bueno, J., Landi Degl'Innocenti, E., & Collados, M. 2006, *ApJ*, 642, 554

Okamoto, T. J., Tsuneta, S., Berger, T. E., *et al.* 2007, *Science*, 318, 1577

Orozco Suárez, D., Asensio Ramos, A., & Trujillo Bueno, J. 2012, *ApJ*, 761, L25

Orozco Suárez, D., Asensio Ramos, A., & Trujillo Bueno, J. 2013, *A&A*, in preparation

Paletou, F. & Aulanier, G. 2003, in Solar Polarization Workshop 3, ed. J. Trujillo Bueno & J. Sánchez Almeida, ASP Conf. Series, Vol. 236 (Astron. Soc. of the Pacific, San Francisco), p. 458

Panasenco, O., Martin, S. F., Velli, M., & Vourlidas, A. 2012, in Solar Dynamics and Magnetism from the Interior to the Atmosphere, eds. R. Komm, A. Kosovichev, D. Longcope, & N. Mansour (Springer, Dordrecht)

Panesar, N. K., Innes, D. E., Tiwari, S. K., & Low, B. C. 2013, *A&A*, 549, A105

Pneuman, G. W. 1983, *Sol. Phys.*, 88, 219

Régnier, S., Walsh, R. W., & Alexander, C. E. 2011, *A&A*, 533, L1

Schmieder, B., Tziotziou, K., & Heinzel, P. 2003, *A&A*, 401, 361

Schmit, D. J., Gibson, S. E., Tomczyk, S., *et al.* 2009, *ApJ*, 700, L96

Schmit, D. J. & Gibson, S. E. 2013, *ApJ*, 770, id. 35

Sheeley, N. R., Jr., Martin, S. F., Panasenco, O., & Warren, H. P. 2013, *ApJ*, 772, article id. 88

Su, Y., Wang, T., Veronig, A., Temmer, M., & Gan, W. 2012, *ApJ*, 756, L41

Su, Y., van Ballegooijen, A. A., & Golub, L. 2010, *ApJ*, 721, 901

Tandberg-Hanssen, E. 1995, The nature of solar prominences, Astrophys. Space Sci. Lib., Vol. 199 (Dordrecht: Kluwer Academic Publishers)

Trujillo Bueno, J., Landi Degl'Innocenti, E., Collados, M., Merenda, L., & Manso Sainz, R. 2002, *Nature*, 415, 403

van Ballegooijen, A. A. Priest, E. R., & Mackay, D. H. 2000, *ApJ*, 539, 983

van Ballegooijen, A. A. & Cranmer, S. R. 2010, *ApJ*, 711, 164

Wang, Y.-M. 1999, *ApJ*, 520, L71

Wang, Y.-M. 2001, *ApJ*, 560, 456

Wang, Y.-M. & Muglach, K. 2007, *ApJ*, 666, 1284

Wang, Y.-M. & Stenborg, G. 2010, *ApJ*, 719, L181

Yeates, A. R. & Mackay, D. H. 2012, *ApJ*, 753, L34

Yelles Chaouche, L., Kuckein, C., Martinez Pillet, V., & Moreno-Insertis, F. 2012, *ApJ*, 748, 23

Zirker, J. B., Martin, S. F., Harvey, K., & Gaizauskas, V. 1997, *Sol. Phys.*, 175, 27